Aerosol and Air Quality Research, 16: 653–664, 2016

ISSN: 1680-8584 print / 2071-1409 online
doi: 10.4209/aaqr.2015.05.0320

Impact of Long-Range Transported African Dust on Cloud Water Chemistry at a Tropical Montane Cloud Forest in Northeastern Puerto Rico

Carlos J. Valle-Díaz[1,2], Elvis Torres-Delgado[1], Stephanie M. Colón-Santos[2], Taehyoung Lee[3], Jeffrey L. Collett Jr.[4], William H. McDowell[5], Olga L. Mayol-Bracero[1*]

[1] *Department of Environmental Science, University of Puerto Rico, San Juan, Puerto Rico, USA*
[2] *Department of Chemistry, University of Puerto Rico, San Juan, Puerto Rico, USA*
[3] *Department of Environmental Science, Hankuk University of Foreign Studies, Seoul, Korea*
[4] *Department of Atmospheric Science, Colorado State University, Fort Collins, Colorado*
[5] *Department of Natural Resources and the Environment, University of New Hampshire, Durham, New Hampshire*

ABSTRACT

Bulk and drop size fractionated cloud water was collected at a Caribbean tropical montane cloud forest (TMCF) in northeastern Puerto Rico in the summer months of 2010–2012 and winter months of 2011 as part of the *Puerto Rico African Dust and Cloud Study* (PRADACS). We studied how cloud water chemistry in a Caribbean TMCF was affected by long-range transported African dust (LRTAD). Using HYSPLIT trajectories and enrichment factor analysis, the air masses influencing clouds at Pico del Este were identified as dust, marine, and dust with anthropogenic influence. Samples were analyzed for pH, conductivity, water-soluble ions, and metals. Na^+ and Cl^- comprised the main water-soluble ions (60–80%) suggesting a strong marine influence. A 0.1–10% contribution of anthropogenic (nss-SO_4^{2-}) and 0.2–13% contribution of mineral dust (nss-Ca^{2+}) sources to the cloud chemical composition was observed. Primary aerosols (i.e., mineral dust and sea-salt) were enriched in large cloud water droplets (LCWD) and secondary aerosols (i.e., anthropogenic particles) were enriched in small cloud water droplets (SCWD). As a result, pH was found to be higher in LCWD due to the neutralizing capacity of nss-Ca^{2+} and lower in SCWD due to the presence of acidifying species (nss-SO_4^{2-}, NO_3^-, and organic acids). Fe and Al, indicators for mineral dust were similarly distributed across the cloud droplet size spectrum. Our results show that LRTAD events modulate bulk and size-fractionated cloud water chemistry, potentially influencing cloud microphysical properties and processes.

Keywords: Sahara desert; Desert dust; Rainforest; Cloud processing.

INTRODUCTION

Clouds and precipitation are potential sources of water and nutrients in ecosystems, and are particularly important in tropical montane cloud forests (TMCFs) (Bubb *et al.*, 2004; Bruijnzeel *et al.*, 2010). These forests are unique among terrestrial ecosystems in the sense that they are strongly linked to regular cycles of cloud formation and are known to strip water from the wind-blown fog and clouds, thus adding to the water supplies available downstream (Stadtmüller and Agudelo, 1990; Still *et al.*, 1999). TMCFs cover approximately 500,000 km^2 of tropical mountain ranges, mainly at altitudes between 1200 and 2400 m.a.s.l. (Stadtmüller and Agudelo, 1990). They are known for their vital role in the provision of freshwater, as hotspots of biodiversity associated with very high levels of endemism, and for their high vulnerability to climate change (Lugo and Scatena, 1992; Aldrich *et al.*, 1997; Loope and Giambelluca, 1998). A shift in temperature and precipitation could have serious ecological consequences in these fragile forest ecosystems. Modeling observations suggest that TMCFs are at high risk for changes associated with global warming due to warmer temperatures and higher clouds that are fewer in number (Still *et al.*, 1999). As average temperature increases, optimum habitat for many species may shift them upslope above the highest elevations on a given peak, or where changes may be taking place too quickly for ecosystems and species to adjust and lead them to extinction as in the case of Monteverde Cloud Forest Reserve in Costa Rica (Pounds *et al.*, 1999). The lifting of the cloud base to a level above a TMCF leads to a significant moisture loss, but cloud dynamics and cloud chemistry are poorly described in most TMCFs. There are over 600 TMCFs identified in the world that are exposed to human activities and climate

* Corresponding author.
Tel.: 787-764-0000 Ext. 3430, Fax: 787-772-1481
E-mail address: omayol@ites.upr.edu

change (Bubb *et al.*, 2004). Furthermore, the exponential rise of global industrialization and urbanization involves the generation of manmade aerosols and resulting alteration of the magnitude and intensity of naturally occurring aerosols. TMCFs can be affected by these natural and anthropogenic aerosols that are delivered to these unique ecosystems. Around 15–20 TMCFs are in the Caribbean (Bubb *et al.*, 2004). Particularly during the summer months, significant amounts of mineral dust from the Saharan desert and Sahel regions in Africa arrive to the Caribbean (Prospero, 1999; Prospero and Lamb, 2003; Prospero and Mayol-Bracero, 2013) and can therefore affect these TMCFs. These long-range transported African dust particles (LRTAD) cover a wide latitudinal band, from 5°N to 30°N, in the Northern Tropical Atlantic (NTA) and are believed to be responsible for 10%–20% of the dust concentration in North America (Jones and Moberg, 2003). This dust can also reach South America, northern Europe, and the Middle East (Usher *et al.*, 2003).

High atmospheric loadings of dust particles pose a threat to the environment and climate. As dust travels through long distances, its physical and chemical properties can be modified by processes such as heterogeneous chemical reactions with trace gases, coagulation with other particles, and in-cloud processing (Maring *et al.*, 2003). Dust ages during transport and can mix with aerosols from other sources. The addition of soluble species to the dust can modify its capacity to act as cloud condensation nuclei (CCN) and its optical properties can change when internal mixing occurs (Rosenfeld *et al.*, 2001; Haywood *et al.*, 2008). Understanding the dust's role as CCN and indirect effects on clouds at a regional and global scale requires studies of dust effects on cloud chemistry and physics at sites throughout the world.

The LRTAD chemical composition in cloud water should be characterized to assess its role in cloud formation and processes and to elucidate the aerosol-cloud-precipitation interactions that could have long-term effects on the hydrological cycle and ecosystems of areas with the influence of LRTAD. Puerto Rico's TMCF of Pico del Este (PE), sometimes also known as East Peak (English translation), located in the northeastern part of the island, serves as a natural laboratory for the study of the impact of aerosols on the physics and chemistry of clouds. Studies at PE can apply to other regions of the world to extrapolate the impact of LRTAD events on cloud water chemistry. Though previous studies have characterized the chemistry of clouds at PE (Martens and Harriss, 1973; Weathers *et al.*, 1988; Asbury *et al.*, 1994; Allan *et al.*, 2008; Gioda *et al.*, 2008, 2009; Reyes-Rodriguez *et al.*, 2009; Gioda *et al.*, 2011, 2013), none have characterized it by cloud droplet size nor have they focused on determining the impact of African dust events on Caribbean cloud water chemistry. This paper addresses how LRTAD events modulate cloud water chemistry in the Caribbean as a starting point to develop a better understanding of the impact of African dust particles on clouds and climate in regions that contain TMCFs. This study is part of the *Puerto Rico African Dust and Cloud Study* (PRADACS, http://pradacs.catec.upr.edu/), a collaborative project with researchers from USA, Europe and Latin America that aimed to determine how the chemical and physical properties of aerosols, clouds, and rainwater in the TMCF of PE are changed by the input of LRTAD particles. Results presented here will ultimately contribute to the PRADACS goal of better understanding the potential impacts of LRTAD on the Caribbean region.

METHODS

Sampling Site

Cloud water was sampled at PE (18°16' N, 65°45' W), in the Luquillo Experimental Forest (LEF), part of El Yunque National Forest (EYNF). The LEF, administered by the USDA Forest Service and located in the windward eastern portion of the island, is one of the wettest areas on the island and in the region. This ecosystem is characterized by short stature trees, endemic rich flora, saturated soils (Scatena, 1995), and slow rates of recovery following disturbance (Byer and Weaver, 1977; Weaver, 1990; Olander *et al.* 1998). In addition to rainfall, this forest gains between 2 and 4 mm of water from cloud droplet deposition on plants for each 25 mm of rainfall, or about 10% of average annual rainfall (Weaver, 1972). PE's elevation (1051 m.a.s.l.) sits above the cloud condensation level and thus facilitates the study of warm clouds without the need for aircraft and the related complexity and costs. Mean annual precipitation at PE is > 5000 mm yr^{-1} (García-Martinó *et al.*, 1996). The influence of local pollution on the site is minimal. Furthermore, PE is the location of an air traffic control station from the Federal Aviation Administration, which restricts access to the site from the general public. Only authorized personnel are allowed to enter PE, which minimizes anthropogenic emissions during sampling periods. This site is ideal for studies of aerosol-cloud-precipitation interactions, gas-phase chemistry, weather and climate observations, global and regional model comparisons to mountain sites, and tests of new sampling techniques. This site has been a hotspot for local, national, and international researchers to study aerosol-cloud-precipitation interactions and mountain hydrology in the Caribbean (Eugster *et al.*, 2006; Allan *et al.*, 2008; Gioda *et al.*, 2008; Reyes-Rodríguez *et al.*, 2009; Gioda *et al.*, 2013; Spiegel *et al.*, 2014; Fitzgerald *et al.*, 2015).

Sampling Strategy

The PRADACS campaigns were conducted during the summer months of 2010–2012 and winter months of 2010–2011. We relied on forecasting models and satellite imagery to identify incoming dust events arriving at PR and to prepare for sampling. These included satellite aerosol optical thickness (AOT) and real color images from MODIS (http://modis-atmos.gsfc.nasa.gov/MOD04_L2/), satellite images from the Saharan Air Layer (SAL - http://tropic.ssec.wisc.edu/real-time/salmain.php?prod=splitE&time), dust forecasting systems from the Navy Aerosol Analysis and Prediction System (NAAPS - http://www.nrlmry.navy.mil/aerosol/) and the SKIRON model (University of Athens, Greece - http://forecast.uoa.gr/), and weather forecasts provided by

the National Weather Service.

Cloud water samples were collected using an aluminum version of the compact single-stage Caltech Active Strand Cloud Water Collector Version 2 (Al-CASCC2) and a size fractioning 2-stage collector (sf-CASCC). Both Al-CASCC2 and sf-CASCC are active collectors that use a fan to draw droplet-laden air across a bank of Teflon collection surfaces as described by Demoz *et al.* (1996). The cut-off diameter of the Al-CASCC2 is 3.5 μm and for the sf-CASCC it is 17 μm and 4 μm. The collectors were placed at approximately 2-m height in a large open area (~300 m^2) with no nearby trees to avoid splash or throughfall contamination (Gioda *et al.*, 2008; Reyes-Rodríguez *et al.*, 2009). The samplers were exposed just before an event and removed immediately after. Prior to sample collection, the collectors were rinsed thoroughly with Milli-Q water. Field blank samples were obtained by spraying the collectors with Milli-Q water. Cloud water samples, ranging between 25 and 800 mL of sample volume, were collected for 1–3 hours during the day depending on the visibility at the site. If visibility was higher than 200 m, or a precipitation event started, the collector was turned off. Samples collected with the Al-CASCC2 are referred to as bulk cloud water (BCW), and those collected with the sf-CASCC are large cloud water drops (LCWD) for the first stage and small cloud water drops (SCWD) for the second stage. BCW collected with the Al-CASCC2 is representative of the entire cloud drop size distribution (Demoz *et al.*, 1996).

Chemical Analysis

Conductivity (WTW Cond 3150i conductometer) and pH (AB 15, Fisher Scientific pH meter) of the collected cloud water were measured in the field, immediately after sampling. The pH meter was calibrated with pH 4.01, 7.00, and 10.00 buffers. All the samples for cloud and rain water were divided into aliquots of 25–40 mL for analysis of water-soluble ions and metals. Samples separated for trace metals analysis were preserved with nitric acid (pH < 2). The samples were transported in coolers with ice at around 4°C and stored in a freezer in the laboratory at –18°C until analysis. Sample handling and aliquot volumes were adapted from previous work performed in our research laboratory (Gioda *et al.*, 2008; Reyes-Rodríguez *et al.*, 2009; Gioda *et al.*, 2013).

Water-soluble ions were determined using an ion chromatograph (Dionex ICS 1000) with conductivity detection. Anions and organic acids were measured using an ION Pac AS22 column with an eluent of 4.5 mM Na_2CO_3 and 1.4 mM $NaHCO_3$. Cations (except NH_4^+) were measured with an ION Pac CS12 column with an eluent of methanesulfonic acid (30 mM). NH_4^+ was determined by the phenate method using a robotic Smartchem colorimetric analyzer (Unity Scientific). Trace metals were determined by inductively coupled plasma (ICP Model Ciros CCD) with optical emission detection. IC analyses were conducted at the Water Quality Analysis Laboratory, University of New Hampshire, and ICP analyses were conducted at the International Institute of Tropical Forestry – United States Department of Agriculture Forest Service (IITF-USDAFS) located in Puerto Rico. Precision of measurements for both ions and metals were less than 5% relative standard deviation (RSD).

The measured water-soluble ions include inorganic cations (Na^+, K^+, NH_4^+, Ca^{2+}, and Mg^{2+}) and anions (Cl^-, NO_3^-, and SO_4^{2-}) and organic acids (formate, acetate, and oxalate). For simplicity the sum of the three organic acids will be designated as OA. HCO_3^- was calculated using the assumed equilibrium of background $CO_{2(g)}$ concentrations in water, whereas CO_3^{2-} was not calculated since below pH 9 the concentration is virtually zero and all samples had pH values less than 7.5 (Manahan, 2000). Sea salt (ss) and non-sea-salt (nss) fractions of SO_4^{2-}, K^+, and Ca^{2+} were calculated for each sample using Na+ as the sea-salt tracer (Wilson, 1975). The acid-soluble forms of trace elements studied included Al, Ca, Fe, K, Mg, Na, and S. Other ions (i.e., F^-, Br^-, NO_2^-, Li^+, PO_4^{3-}) and elements (Mn and P) were analyzed, but were found to be below the instrument detection limits and are not included for discussion in this article. Table 1 shows the detection limits of all chemical species analyzed in this study. The limit of detection was based on three times the standard deviations of blanks from the collectors. All species, except Na^+, K^+, Cl^-, Mg^{2+}, Ca^{2+}, SO_4^{2-} were below detection limits at times because our sampling site is quite clean under the trade-winds influence. Organic acids were below detection limit in many samples due to the low organic carbon found in cloud water at the site.

Dust Event Characterization Scheme

To determine the impact of LRTAD events on cloud water chemistry, a comprehensive characterization of air masses arriving at PR is essential in order to determine which days during the PRADACS campaign PE was influenced by dust events. An important advantage of this exercise is that other air masses can be identified that may contain contributions from various anthropogenic and natural sources (e.g., southeastern islands, United States, biomass burning from Africa, and/or volcanic ash from the island of Montserrat located southeast of PR amongst the British islands). Results on the chemical composition presented here will be compared with classified air masses in order to assess the impact of LRTAD events on cloud water chemistry.

The origin of air masses was determined using the HYSPLIT_4 (HYbrid Single Particle Lagrangian Integrated Trajectories) model (Draxler and Hess, 1998). Hourly 7-day back trajectories at 1000 AGL for the sampling periods were run to acquire a qualitative indication of the main sources of particles arriving at PE. All trajectories were displayed as a trajectory frequency plot by creating an arbitrary grid of 0.5° grid resolution using GDAS with nested NAM12 meteorology over the computational domain and then counting the number of trajectory intersections (whether once or multiple) over each grid point and dividing by the total number of trajectories. Wind direction collected with the Davis Weather Station was used to generate wind roses to observe wind speed and direction at PE and complement it with HYSPLIT analysis.

Bulk chemical analysis of the collected cloud water allows the identification of potential sources by enrichment

Table 1. Detection limits of water-soluble ions and soluble trace metals.

Chemical Species	Detection Limit (mg L^{-1}) – Blanks from Collectors
Cl^-	1
NO_3^-	0.2
SO_4^{2-}	0.2
Acetate	0.2
Formate	0.1
Oxalate	0.05
Na^+	0.7
K^+	0.04
Mg^{2+}	0.3
Ca^{2+}	0.2
NH_4^+	0.04
Al	0.9
Ca	0.5
Fe	0.3
K	0.6
Mg	0.3
Na	2
S	0.4

factor (EF) analysis, calculated by comparing the ionic ratios in cloud water to ratios of elements present in the Earth's crust and seawater. Ca^{2+} was used as the reference element for soil and Na^+ as the reference element for marine sources using the following equations:

$$EF_{seawater} = \frac{\left(\frac{X}{Na^+}\right)_{cloudwater}}{\left(\frac{X}{Na^+}\right)_{seawater}} \quad (1)$$

$$EF_{soil} = \frac{\left(\frac{X}{Ca^{2+}}\right)_{cloudwater}}{\left(\frac{X}{Ca^{2+}}\right)_{soil}} \quad (2)$$

where X is the concentration of the ion, X/Na^+ of seawater is the ratio reported for seawater (Keene *et al.*, 1986) and X/Ca^{2+} of soil is the ratio reported for crustal origin (Taylor, 1964). Concentrations used in the calculation of EF for seawater are expressed in μeq L^{-1} and EF for soil in ppm (mg L^{-1}). The calculated EFs were used to approximate the marine and crustal contributions of different ionic species in cloud water by their respective sea salt fraction (SSF) and crustal fraction (CF), using the following equations:

$$\%SSF = 100 \times \frac{\left(\frac{X}{Na^+}\right)_{seawater}}{\left(\frac{X}{Na^+}\right)_{cloudwater}} \quad (3)$$

$$\%CF = 100 \times \frac{\left(\frac{X}{Ca^{2+}}\right)_{soil}}{\left(\frac{X}{Ca^{2+}}\right)_{cloudwater}} \quad (4)$$

To identify what air masses influenced collected samples, three categories were used: (1) a sample yielding %SSF less than 100 for Ca^{2+} was considered to be influenced by dust, (2) if the %SSF did not yield less than 100, the samples were considered to be of background marine aerosols. (3) The anthropogenic fraction (%AF) of SO_4^{2-} was calculated by subtracting %SSF and %CF from 100%. Even though the %CF refers to sulfur in its elemental form (S), it was assumed that all sulfur was oxidized to SO_4^{2-}. Therefore if the %AF of SO_4^{2-} yielded above 0, the sample was classified as influenced by anthropogenic particles. The air masses determined for each cloud water sample through chemical measurements were confirmed with individually calculated HYSPLIT trajectories for every cloud sampling period.

Quality Assurance and Control

Conductivity was calculated using the following equation in order to compare results of IC analyses with the conductivity measured in the field. Results were expressed as percentage of conductivity difference (%CD) of calculated and measured conductivity.

$$C_{calc} = \sum \lambda_i c_i \quad (5)$$

C_{calc} is the calculated conductivity, λ_i is the equivalent ionic conductance at infinite dilution at a certain temperature, and c_i is the individual ion concentration. Ions used to calculate C_{calc} were: Cl^-, NO_3^-, SO_4^{2-}, formate, acetate, oxalate, HCO_3^-, Na^+, H^+, NH_4^+, K^+, Mg^{2+} and Ca^{2+}. A %CD average of (12 ± 13) % was obtained for bulk cloud water, (11 ± 9) % for coarse cloud water droplets, and (15 ± 8) % for fine cloud water droplets. Approximately 60% of the samples had a good agreement with conductivity measured in the field and total ion concentrations (< 10 %CD). Around 30% of the samples were within 12–30 %CD. A few samples had high %CD ranging from 30% to 80% that

could be attributed to analytical errors, other water-soluble species not determined nor included to calculate C_{calc}, or losses of certain species into the gas phase as a result of reactions or changes in pH. Samples that exceed 30 %CD were excluded from the data set.

A ≤ 15% difference in ionic balance for samples having ion concentrations of 100 μeq L^{-1} and above was used as criteria for an acceptable ionic balance (Peden, 1983). 83% of PRADACS cloud water samples met the quality criteria based on ionic balance. The average anion-to-cation ratio yielded (0.81 ± 0.09) with a strong correlation between them (r^2 = 0.97), suggesting a good electric charge balance between both ionic groups.

To verify statistical similarity and differences among the sample types within varying air masses, analysis of variance (ANOVA) and Tukey-HSD (honest significant difference) tests at the 95% confidence level were performed with the R-Console program (Version 2.15.0, 2012). A p-value of less than 0.05 was used to determine statistical difference amongst the data sets.

RESULTS AND DISCUSSION

Air Masses

HYSPLIT trajectory frequency at 1000 AGL for the summer periods (Fig. 1(a)) shows that air masses arriving at PE come primarily from northeast and east, setting the path to receive African dust plumes that travel through the Atlantic Ocean. Marine aerosols are expected to be present at all times due to PR's proximity to the ocean. The fraction of the air masses crossing the southeastern islands might be the cause of anthropogenic pollution mixed with the incoming marine and dust air masses. Other trajectories (Fig. 1(b)), relatively few in number, come from North America and are a source of anthropogenic pollution. These were present only during the winter periods of our study. Wind direction data related very well with our trajectory analysis where winds came between ENE and ESE at speeds ranging from 0.5–5.7 m s^{-1}. Air masses passing the island of Montserrat could have provided volcanic ash in our samples, but reports from the Montserrat Volcanic Observatory (www.mvo.ms) did not mention any volcanic ash venting during our sampling campaigns. During the input of dust air masses, we also observed orange colored sand deposits in the cloud water samples due to the presence of iron oxides.

EF analyses show that for the 94 cloud water samples, 54 were influenced by dust events, 15 were mainly of background marine aerosols, and 16 were influenced by dust events with anthropogenic influence. The remaining 9 samples did not have water-soluble ion data to classify through EF analysis. Dust air masses, regardless of being mixed with anthropogenic influence or not, were confirmed by weather forecasts, increased AOT values from MODIS satellite images, arrival of dust plumes shown in SAL images, and SKIRON and NAAPS modeled dust concentrations over PR. For the remaining part of the paper, we will discuss the results on the basis of three air mass classifications: Dust, Marine, (Dust + Anthropogenic).

Water Soluble Ions in Cloud Water

Average concentrations of water-soluble ions present in cloud water samples under the influence of various air masses are shown in Figs. 2(a)–2(b). Na^+ and Cl^- represent 75% (BCW and LCWD) and 63% (SCWD) of the overall composition of water-soluble ions. Species such as Mg^{2+}, SO_4^{2-}, and Ca^{2+} contributed approximately 20% of the total. Calculating the non-sea salt (nss) fraction of SO_4^{2-} and Ca^{2+}, using the concentration of Na^+ as a reference for marine

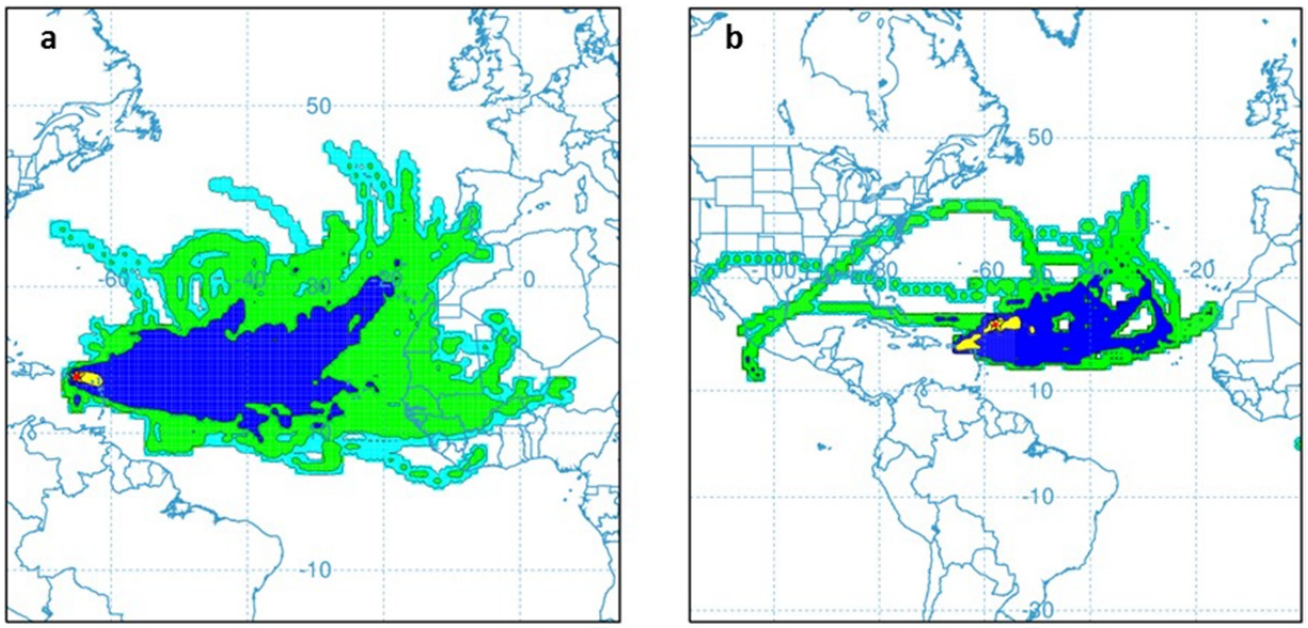

Fig. 1. Frequency plot of individual backward trajectories using HYSPLIT (Draxler and Hess, 1988) at 1000 AGL for the sampling periods – (a) summer and (b) winter. Light blue = > 0.1%, Green = > 1%, Blue = > 10%, Yellow = > 100% of trajectories. 222 trajectories were calculated for the summer periods and 27 trajectories were calculated for the winter periods.

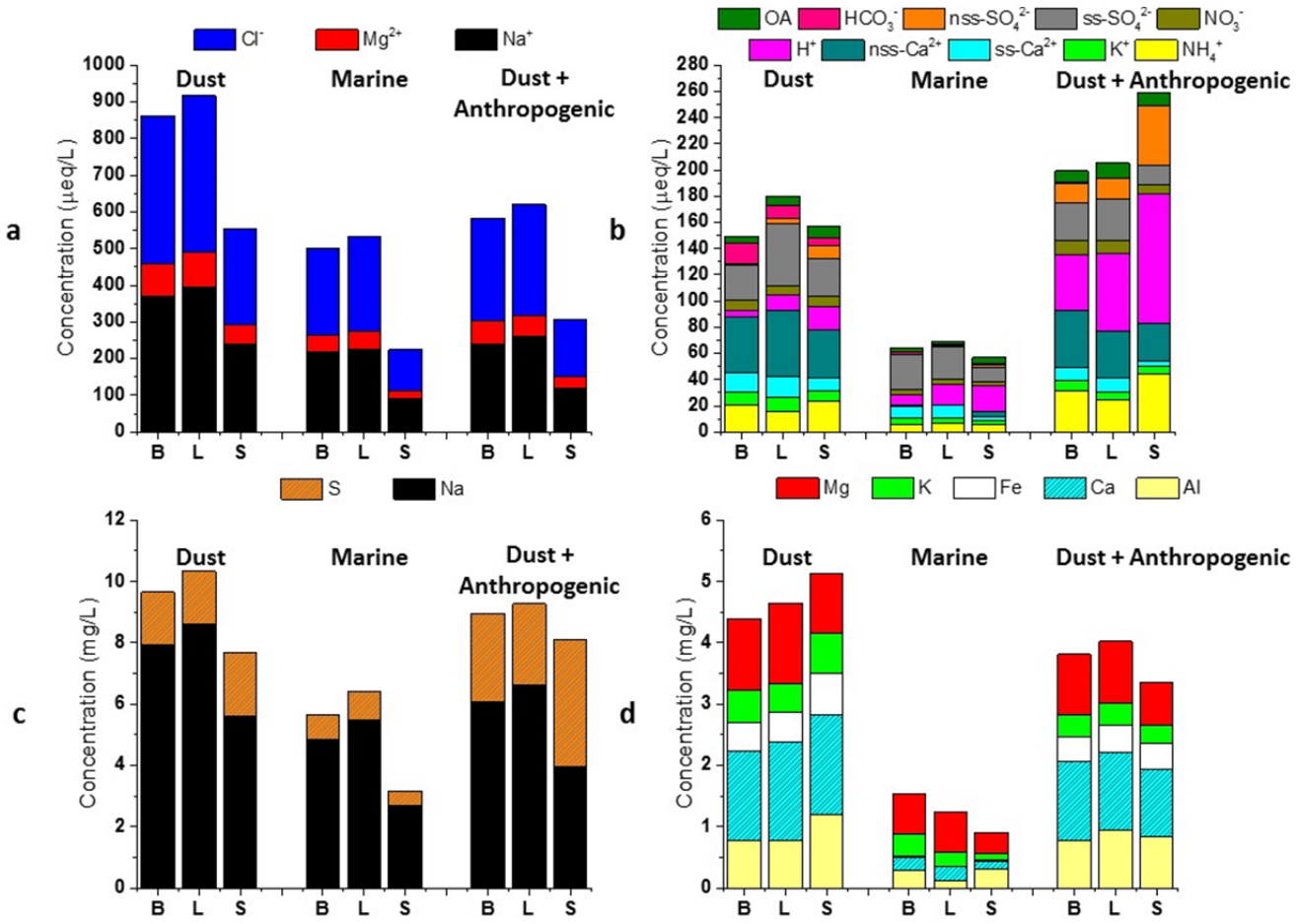

Fig. 2. Stacked bar graphs of average concentrations of Na^+, Cl^-, and Mg^{2+} (a), rest of water-soluble ions studied (b), Na and S (c), and rest of trace metals studied (d) in cloud water under the influence of different air masses. B = bulk cloud water, L = large cloud water drops, and S = small cloud water drops. Concentrations of water-soluble ions expressed in μeq L^{-1} and trace metals expressed in mg L^{-1}.

origin (Wilson, 1975), a contribution of nss-SO_4^{2-} and mineral dust (nss-Ca^{2+}) sources to the cloud chemical composition is observed. Nss-SO_4^{2-} can originate from anthropogenic production of SO_2 and dimethylsulfide emissions from the ocean. Very small amounts of nss-SO_4^{2-} were observed in cloud water samples influenced by marine air masses, thus the nss-SO_4^{2-} is essentially from anthropogenic origin. The less dominant ions that composed the remaining 5–15% were NH_4^+, H^+, K^+, OA, NO_3^-, and HCO_3^-. Tables S1–S3 in the supplementary material describe the values (minimum, maximum, average, standard deviation, and number of samples) for each chemical species in the cloud water samples under the influence of various air masses.

Table 2 summarizes the correlations between the water-soluble ions observed in BCW. The main five species observed (i.e., Na^+, Cl^-, Mg^{2+}, SO_4^{2-}, and Ca^{2+}) come mainly from sea salt and reflect the proximity of the sampling site to the ocean. The high correlation of Na^+ and Cl^- (r = 0.99) indicates a common marine source, and other sea-salt components i.e., K^+, Mg^{2+}, and Ca^{2+} also correlated very well with Na^+ (r = 0.92, 0.99, and 0.82, respectively) and Cl^- (r = 0.92, 0.98, and 0.83, respectively). K^+, Mg^{2+} and Ca^{2+} had correlations over 0.90 with each other suggesting the possible contribution of material of crustal origin, but K^+/Na^+, and Mg^{2+}/Na^+ ratios were similar to those in seawater whereas Ca^{2+}/Na^+ ratios were higher, suggesting a mix of crustal and marine sources. Na^+, K^+, Mg^{2+}, and Ca^{2+} showed moderate correlations with NO_3^- (r = 0.59, 0.65, 0.63, and 0.69, respectively) and weak correlations with nss-SO_4^{2-} (r = 0.27, 0.41, 0.26, and 0.19), which suggests a preferential reaction of mineral components usually rich in carbonate and/or sea salt with HNO_3. A relatively good correlation (r = 0.65–0.75) also exists between NH_4^+ and Na^+, K^+, Mg^{2+}, and Ca^{2+} even though its main source is from anthropogenic origin, but natural decomposition of organic matter in the TMCF provides a biogenic source of NH_4^+ that can be mixed with marine aerosols due to the proximity of PE to the ocean (Weathers *et al.*, 1988). H^+ ions had the best correlation with nss-SO_4^{2-} (r = 0.84), from which we conclude that SO_4^{2-} is the main acidifying species in PE cloud water. NH_4^+ correlated relatively well with nss-SO_4^{2-} (r = 0.63) and NO_3^- (r = 0.68), suggesting either a common source, most likely anthropogenic, and/or reflecting the importance of sulfuric acid and nitric acid neutralization by ammonia in aerosols or cloud water. NH_4^+ is often associated with SO_4^{2-} and NO_3^- as $(NH_4)_2SO_4$,

Table 2. Correlation coefficients among water-soluble ions in bulk cloud water samples.

	Cl^-	NO_3^-	ss-SO_4^{2-}	nss-SO_4^{2-}	HCO_3^-	OA	Na^+	H^+	NH_4^+	K^+	Mg^{2+}	ss-Ca^{2+}	nss-Ca^{2+}
Cl^-	1	0.58	0.99	0.28	0.53	0.39	0.99	–0.17	0.67	0.92	0.98	0.99	0.73
NO_3^-		1	0.59	0.58	0.39	0.29	0.59	0.17	0.68	0.65	0.63	0.59	0.68
ss-SO_4^{2-}			1	0.27	0.53	0.35	1	–0.18	0.66	0.92	0.99	1	0.72
nss-SO_4^{2-}				1	–0.38	0.42	0.27	0.84	0.63	0.41	0.26	0.27	0.16
HCO_3^-					1	–0.05	0.53	–0.30	0.26	0.51	0.52	0.53	0.62
OA						1	0.35	0.30	0.57	0.38	0.37	0.35	0.28
Na^+							1	–0.18	0.66	0.92	0.99	1	0.72
H^+								1	0.28	–0.08	–0.17	–0.18	–0.14
NH_4^+									1	0.70	0.70	0.66	0.71
K^+										1	0.92	0.92	0.79
Mg^{2+}											1	0.99	0.76
ss-Ca^{2+}												1	0.72
nss-Ca^{2+}													1

NH_4HSO_4 and NH_4NO_3. Previous studies from Gioda *et al.* (2008); Reyes-Rodríguez *et al.* (2009) and Gioda *et al.* (2013) showed similar trends of contributing species and correlations in bulk cloud water at PE.

No size-fractionated cloud water chemistry has been reported in the literature for Puerto Rico, but studies from other regions show that aerosols in large cloud water droplets are sometimes associated with sea salt and/or mineral dust particles, while small cloud water droplets contain secondary aerosols that are more acidic in aqueous media (e.g., Collett *et al.*, 1994; and Bator and Collett, 1997). Large particles that activate as cloud droplets further grow through collision and coalescence of smaller droplets, whereas small particles that activate are grown through condensation processes, but not enough to catch up in size to the activated larger particles. Therefore, when aerosol particles are activated as cloud droplets, it is expected that they retain to some extent the chemical variation across the cloud droplet size distribution. Although the trend described by the authors applies for cloud water sampled at least near the cloud base, the trend has also been observed in a wide variety of conditions and cloud types. Results from Figs. 2(a)–2(b) are in agreement with the observations from the aforementioned studies given that Na^+, Cl^-, K^+, Mg^{2+}, ss-SO_4^{2-}, ss-Ca^{2+}, and nss-Ca^{2+} are enriched in LCWD and nss-SO_4^{2-}, produced by secondary processes, is enriched in SCWD.

NH_4^+ and OA found in cloud samples both originate from primary and secondary emissions. Primary emissions most likely occurred as gas phase molecules derived from the forest and secondary emissions probably from anthropogenic emissions originating from Africa and the Southeastern Islands. NH_4^+ was enriched in LCWD under clean background conditions, which could be of biogenic origin, and was enriched in SCWD under the influence of dust events and dust events with anthropogenic influence. On average NO_3^-, was enriched in LCWD. This could be due to the incorporation of HNO_3 into mineral dust particles.

Low molecular weight carboxylic acids are ubiquitous in the atmosphere in a large range of environments, but originate mainly through anthropogenic and biogenic emissions and chemical transformations of precursor species (Chebbi and Carlier, 1996). In agreement with Chebbi and Carlier (1996), formic and acetic acid were the predominant carboxylic acids in cloud water. Oxalate, a marker sometimes used as evidence for cloud processing (Yu *et al.*, 2004), comprised an average of (33 ± 25) % of the OAs measured.

Relative to background conditions, total ion concentrations increased in dust events by 185% on BCW and LCWD, and 245% on SCWD, whereas total ion concentrations in dust events mixed with anthropogenic influence increased 140% for BCW and LCWD and 201% in SCWD. In addition, total ion concentrations in LCWD were 140–205% higher than in SCWD, depending on the air mass. Approximately 25–30% of the total K^+ were comprised of nss-K^+ in LCWD and 38–50% in SCWD during dust events and dust events mixed with anthropogenic influence. Increase of K^+ in SCWD during dust events suggest possible influence from biomass burning particles from Africa that can mix with dust particles during transport.

Trace Metals in Cloud Water

Average concentrations of trace soluble elements present in cloud water samples varied by air mass origin (Figs. 2(c)–2(d). Na and S were the main species, representing 73% of the BCW and LCWD, and 70% of the SCWD with respect to the overall composition of soluble trace elements. The remaining 30% corresponding to Ca and Mg, also predominant elements, followed by Al, Fe, and K. Al and Fe are of crustal origin and correlated very well during dust events (r = 0.96) and dust events mixed with anthropogenic pollution (r = 0.97). Fe was not detected in cloud water samples under background conditions. Ca and Fe showed good correlation during dust events (r = 0.78) and dust events mixed with anthropogenic pollution (r = 0.86), but this relationship was not as strong as that for Al with Fe because of the added contribution of Ca from marine origin.

Compared to background conditions, total elemental concentrations in dust events increased by 195% in BCW and LCWD, and 315% in SCWD, whereas dust events mixed with anthropogenic influence increased by 178% in BCW, 174% in LCWD, and 282% in SCWD. In addition, total elemental concentrations in LCWD were 116–188% higher than in SCWD, depending on the air mass. As observed in Figs. 2(c)–2(d), Na, Mg, Ca, K, and S showed similar trends

amongst cloud droplet size mode in comparison to their ionic forms. During dust events, whether mixed with anthropogenic pollution or not, both Al and Fe appear to be similarly distributed across the cloud droplet size spectra, suggesting a degree of mixing with sea salt and/or anthropogenic particles during long-range transport and differences in the mineralogy of mineral dust particles arriving over time at the site.

Because acid-soluble metals represent the total amounts of elements and water-soluble ions refer to the dissolved fraction, average concentrations (mg L^{-1}) of acid-soluble trace elements and water-soluble ions [Ca (Ca^{2+}), K (K^{+}), Mg (Mg^{2+}), and Na (Na^{+})] were compared to observe how much undissolved material remained. 5–30% of Ca, 15–50% of K, and 7–25% of Mg remained undissolved in cloud water, while only less than 10% of Na was undissolved. Most of the Na is of marine origin. Ca, K, and Mg are present in marine aerosols, but the contribution of the added mineral dust particles is highly likely to affect its solubility in water.

pH, Conductivity, and Charge Balance

In the absence of polluted air masses, the pH of cloud water is around 5.6 due to the equilibrium of atmospheric CO_2 in water (Manahan, 2000). Measuring pH of cloud water under the influence of different air masses can provide insight on chemical species involved in the acidification or neutralization of the cloud water itself. The pH of BCW samples ranged from 3.97 to 7.25 with an average of 4.91. In size fractionated cloud water samples, pH in LCWD ranged from 3.82 to 7.09 with an average of 4.64, while SCWD pH ranged from 3.61 to 7.05 with an average of 4.46. BCW collected with the Al-CASCC2 represents an approximate volume-weighted average of the concentration of both stages of the sf-CASCC. Overall, averaged cloud water pH values are commonly reported for clouds studied in marine influenced environments (Weathers *et al.*, 1988; Collett *et al.*, 2002; Straub *et al.*, 2007; Gioda *et al.*, 2011; Benedict *et al.*, 2012).

In Fig. 3(a) pH values of cloud water under the influence of the classified air masses are shown. When comparing cloud water pH under the influence of marine air masses with pH during dust events, dust events did not significantly increase pH of cloud water. But, dust events that were mixed with anthropogenic particles significantly lowered cloud water pH by the added presence of acidifying species i.e., SO_4^{2-}, NO_3^{-}, and OAs. Cloud water pH during dust events and dust events mixed with anthropogenic particles differed significantly. Samples collected under the influence of dust events that yielded high pH measurements above 6 were usually associated with high nss-Ca^{2+} concentrations from (20–170 μeq L^{-1}), suggesting acid neutralization by crustal components of mineral dust (e.g., Ca^{2+}, K^{+}, and Mg^{2+}). Even though Table 2 indicates that H^{+} is not well correlated with nss-Ca^{2+}, the correlation of H+ with nss-Ca^{2+} improves from –0.14 to –0.34 when considering dust events only. It further increases to –0.50 when considering samples above pH 6. Dust events arrive with different intensities and duration, so if PE would have received more intense events during the sampling campaign, acid neutralizing species may have increased pH values enough to yield statistically significant differences from marine background conditions as seen from previous studies at PE (Reyes-Rodríguez *et al.*, 2009; Gioda *et al.*, 2011). Nonetheless, one can appreciate that pH typically increases during dust events and decreases when anthropogenic pollution is added to the mix. There was no statistical difference between LCWD and SCWD pH within any air mass.

The acidity of cloud water and precipitation depends on the concentration of H^{+} producing species (i.e., SO_4^{2-}, NO_3^{-}, OA, and HCO_3^{-} from dissolved CO_2) and the concentration of alkaline constituents (i.e., NH_4^{+}, and crustal components) that neutralize the acidity in the aqueous media. Using the following equation, the ratios of the concentration of alkaline species to the total concentration of the acid forming species, both in μeq L^{-1}, in individual samples were used to further understand the nature of the acid-base equilibrium occurring in the cloud water under varying air masses.

$$\frac{X_i}{\left[NO_3^-\right]+\left[SO_4^{2-}\right]+\left[OA\right]+\left[HCO_3^-\right]} \quad (6)$$

For X_i equal to NH_4^{+} and any crustal component, the ratio is defined as the neutralization factor (NF) and it is used to evaluate which species is the dominant acidity neutralizer (Possanzini *et al.*, 1988). As for X_i equal to H^{+}, the ratio is defined as the fractional acidity (FA), the capacity of neutralization of cloud water. If FA = 1, it is considered that the acidity generated by the H^{+} producing species is not neutralized (Balasubramanian *et al.*, 2001; Tuncer *et al.*, 2001; Sun *et al.*, 2010).

Table 3 summarizes the calculated NFs for NH_4^{+} and nss-Ca^{2+}, and the fractional acidity of cloud water under the influence of different air masses. Other crustal components (i.e., Na^{+}, K^{+}, and Mg^{2+}) present in the cloud water samples were mainly of marine origin as previously discussed, and thus did not contribute significantly to the acid neutralization of cloud water. On the other hand, Ca^{2+} was a major crustal component found in dust air masses that contributed to neutralizing acidity. Aeolian dust particles contain 5–10% by mass of calcium minerals (e.g., $CaCO_3$) that readily undergo acid-base reactions (Usher *et al.*, 2003; Sullivan *et al.*, 2009). In all cloud water samples acidity was more neutralized during dust events, where Ca^{2+} was the main neutralizing species followed by NH_4^{+} except for dust events mixed with anthropogenic influence where Ca^{2+} and NH_4^{+} similarly contributed to neutralizing pH in SCWD. FA was highest for cloud water influenced by dust events mixed with anthropogenic particles due to the input of acid-forming species. In BCW, FA was below 1 for all air masses giving an impression that all cloud drops are neutralized to some extent, but when comparing cloud droplet sizes, SCWD was not neutralized during background conditions and both LCWD and SCWD were not neutralized during dust events mixed with anthropogenic pollution because H^{+} is not conserved upon mixing. That is, H^{+} concentration in BCW cannot be predicted by volume weighting the H^{+} concentrations in LCWD and SCWD.

Conductivity is proportional to the concentration of all

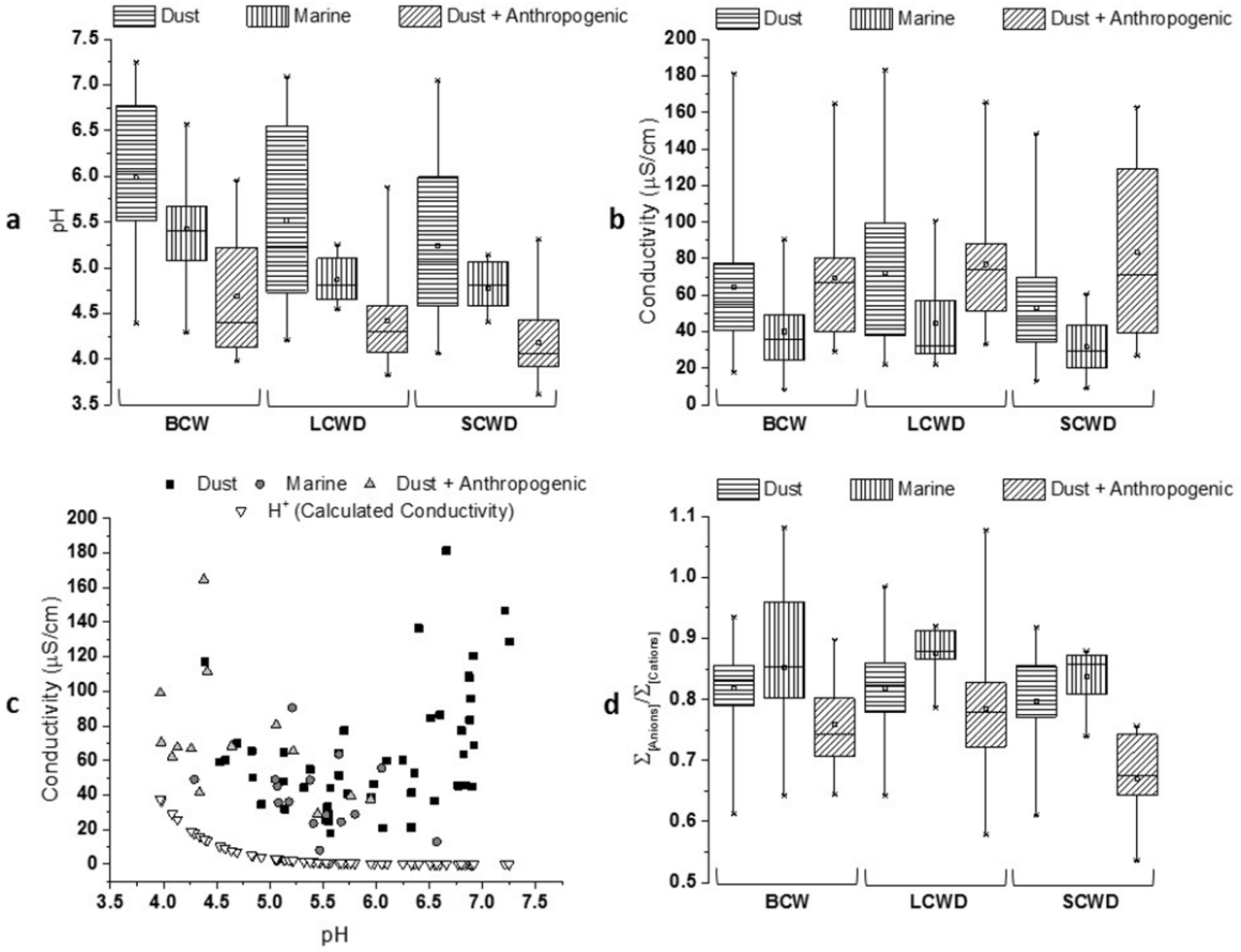

Fig. 3. (a) pH, (b) conductivity, (c) conductivity as a function of pH (for Al-CASCC2 samples only) of cloud water under the influence of different air masses along with the calculated conductivity values for H^+, and (d) anion to cation ratio. BCW = bulk cloud water, LCWD = large cloud water drops, and SCWD = small cloud water drops. Box and whisker plot parameters provided are minimum value, 25th percentile, median, average, 75th percentile, and maximum value.

Table 3. Neutralization factors of NH_4^+ and Ca^{2+} and fractional acidity calculated for cloud water under the influence of varying air masses. Standard deviations of the mean are in parenthesis.

	Air Mass	NF (Ca^{2+})	NF (NH_4^+)	FA
BCW	Dust	0.8 (0.4)	0.4 (0.2)	0.1 (0.2)
	Marine	0.4 (0.1)	0.2 (0.2)	0.2 (0.1)
	Dust + Anthropogenic	0.7 (0.7)	0.5 (0.2)	0.8 (0.7)
LCWD	Dust	0.9 (0.4)	0.3 (0.3)	0.5 (0.6)
	Marine	0.3 (0.1)	0.53 (0.96)	0.8 (0.4)
	Dust + Anthropogenic	0.7 (0.7)	0.4 (0.1)	1.1 (0.8)
SCWD	Dust	0.9 (0.4)	0.5 (0.2)	0.5 (0.5)
	Marine	0.4 (0.2)	0.3 (0.2)	1.1 (0.6)
	Dust + Anthropogenic	0.5 (0.5)	0.5 (0.2)	1.3 (0.8)

water-soluble ions. BCW samples ranged from 8–181 μS cm^{-1} with an average of 61 μS cm^{-1}. The conductivity ranges for size fractionated cloud water samples were similar; 22–183 μS cm^{-1} for LCWD with an average of 69 μS cm^{-1}, and 9–163 μS cm^{-1} for SCWD with an average of 56 μS cm^{-1}. Conductivity measurements of cloud water samples under the influence of various air masses are shown in Fig. 3(b). Conductivity differed significantly in SCWD under marine influenced air masses with SCWD under dust events with anthropogenic influence. During dust events with or without anthropogenic influence, conductivities spanned a larger range relative to clean background conditions. This is to be expected since addition of ions from non-marine sources into the cloud water increases its conductivity. Total

ion concentrations of LCWD were usually larger than SCWD. This should reflect higher conductivity values in LCWD, but was not significantly higher than conductivity in SCWD. A possible reason is that the enrichment of H^+ in SCWD, which has the highest λ_i of all ions, masked the appreciable difference of conductivity in these size-resolved cloud droplets. From Fig. 3(c), we observe that our statement is plausible although dust and sea-salt particles influences overall conductivity at any pH determined in our study.

Calculated anion-to-cation charge ratios of BCW samples ranged from 0.61 to 1.08 with an average of 0.81. In size fractionated cloud water samples, the charge balance ratio in LCWD ranged from 0.58 to 1.08 with an average of 0.82, while SCWD ranged from 0.45 to 0.92 with an average of 0.77. Fig. 3(d) shows the charge balance of cloud water under the influence of various air mass types. Anion-to-cation ratio differed significantly between LCWD and SCWD during dust events mixed with anthropogenic influence. This could have been due to other organic acids that were not measured. Dust mixed with anthropogenic influence has an effect on the charge balance of cloud water, especially amongst cloud droplet size. No statistical difference is observed when comparing based on the type of the air masses, but one can observe that on average the charge balance decreases during dust events and dust events mixed with anthropogenic particles. The decrease in the charge balance was reflected in high %CD values (between 20–30 %CD). Reasons for loss of charge balance could be attributed to chemical species that were not analyzed, loss of organic acids into the gas phase due to a pH effect, insoluble material not ionized in aqueous media, and analytical errors.

CONCLUSIONS

This is the first study examining size-fractionated cloud water chemistry in Puerto Rico, and the data collected allow us to assess how LRTAD events impact cloud water chemistry in the Caribbean. Three different air mass types were identified arriving at Pico del Este (i.e., dust, marine, and dust mixed with anthropogenic influence) through HYSPLIT trajectories and EF analysis of PRADACS cloud water samples.

Cloud water samples were comprised of at least 60% sea-salt ions Na^+, Cl^-, Mg^{2+}, ss-Ca^{2+}, and ss-SO_4^{2-}, reflecting the proximity of the sampling site to the ocean. Nss-SO_4^{2-} and nss-Ca^{2+} were observed during dust events and dust events mixed with anthropogenic pollution. Size-fractionated cloud water chemistry in Puerto Rico was in agreement with studies from other regions in which primary aerosols were often enriched in LCWD and secondary aerosols were often enriched in SCWD. This was reflected in pH and conductivity values. Although no statistical difference between LCWD and SCWD pH within any air mass was observed, pH was higher in average in LCWD, where Ca^{2+} was shown to be the main neutralizing species, and pH was lower in average in SCWD, principally due to the presence of nss-SO_4^{2-}, the main acidifying species in PE cloud water. Concentrations of all acid-soluble trace metals studied increased during dust events, especially Fe and Al, which are direct indicators of mineral dust. Fe and Al showed no preferential enrichment across the cloud droplet size spectrum whereas Na, Mg, Ca, K, and S showed similar trends in enrichment to a cloud droplet size mode relative to their ionic forms.

Because PRADACS cloud water samples were collected during the day, it limits the understanding of size-resolved cloud water chemistry under various conditions at PE (i.e., level of cloud immersion in the forest canopy and meteorological conditions). Further studies are needed to observe size-resolved chemistry at different levels of the cloud between day and night using at least two size-fractionating cloud collectors located at different elevations from the sampling site. Cloud height changes throughout the day in PE and different cloud dynamics can alter the chemistry in the size spectra of cloud drops.

Our results show that LRTAD events impact cloud water chemistry at PE. A diverse and complex dynamic of cloud water chemistry occurs at the site, where differences in cloud formation and aerosol production are possible. Different chemical signatures across the cloud droplet size spectra can produce changes in cloud microphysical properties and processes at the TMCF of PR. This study is the starting point for contributions that will reach the PRADACS goal of better understanding the potential impacts of LRTAD on Caribbean clouds and climate.

ACKNOWLEDGMENTS

We acknowledge the support of NSF AGS 0936879, EAR-0722476 and EAR-1331841. We thank the Luquillo Long-Term Ecological Research Program, the Institute for Tropical and Ecosystem Studies, the El Yunque National Forest, and the Conservation Trust of Puerto Rico (CSJ). Special thanks to the PRADACS team and the Atmospheric Chemistry and Aerosols Research Group at UPR-RP for their help and support (especially to Mr. Félix Zürcher); also to Jody Potter (UNH) for the chemical analysis of water-soluble ions, Mary J. Sanchez from the International Institute of Tropical Forestry USDA Forest Service for the chemical analysis of soluble trace metals, Ricardo Morales, Carlos Estrada, and Frederick N. Scatena, for their help with the weather data, and Ariel Stein for his suggestions regarding HYSPLIT_4.

DISCLAIMER

Reference to any companies or specific commercial products does not constitute an endorsement by the authors.

SUPPLEMENTARY MATERIALS

Supplementary data associated with this article can be found in the online version at http://www.aaqr.org.

REFERENCES

Allan, J.D., Baumgardner, D., Raga, G.B., Mayol-Bracero, O.L., Morales-García, F. and García-García, F. (2008).

Clouds and Aerosols in Puerto Rico - A New Evaluation. *Atmos. Chem.* 8: 1293–1309.

Asbury, C.E., McDowell, W.H., Trinidad-Pizarro, R., Berrios, S. (1994). Solute deposition from Cloud Water to the Canopy of a Puerto Rican Montane Forest. *Atmos. Environ.* 28: 1773–1780.

Bator, A. and Collett Jr., J.L. (1997). Cloud Chemistry Varies with Drop Size. *J. Geophys. Res.* 102: 28071–28078.

Benedict, K.B., Lee, T. and Collet Jr., J.L. (2012). Cloud Water Composition over the Southern Pacific Ocean during the VOCALS Regional Experiment. *Atmos. Environ.* 46: 104–114.

Bruijnzeel, L.A., Mulligan, M. and Scatena, F.N. (2010). Hydrometeorology of Tropical Montane Cloud Forests: Emerging Patterns. *Hydrol. Processes* 25: 465–498.

Bubb, P., May, I., Miles, L. and Sayer, J. (2004). *Cloud Forest Agenda*, UNEP-WCMC, Cambridge, UK.

Byer, M.D. and Weaver, P.L. (1977). Early Secondary Succession in an Elfin Woodland in the Luquillo Mountains of Puerto Rico. *Biotropica* 9: 35–47.

Chebbi, A. and Carlier, P. (1996). Carboxylic Acids in the Troposphere, Occurrence, Sources and Sinks: A Review. *Atmos. Environ.* 30: 4233–4249.

Collett Jr., J.L., Bator, A., Rao, X. and Demoz, B.B. (1994). Acidity Variations across the Cloud Drop Size Spectrum and their Influence on Rate of Atmospheric Sulfate Production. *Geophys. Res. Lett.* 22: 2393–2396.

Collett Jr. J.L., Bator, A., Sherman, D.E., Moore, K.F., Hoag, K.J., Demoz, B.B., Rao, X. and Reilly, J.E. (2002). The Chemical Composition of Fogs and Intercepted Clouds in the United States. *Atmos. Res.* 64: 29–40.

Demoz, B., Collett Jr., J.L. and Daube Jr., B.C. (1996). On the Caltech Active Strand Cloudwater Collectors. *Atmos. Res.* 41: 47–62.

Draxler, R.R. and Hess, G.D. (1998). An Overview of the HYSPLIT_4 Modeling System of Trajectories, Dispersion, and Deposition. *Aust. Meteorol. Mag.* 47: 295–308.

Eugster, W., Burkard, R., Holwerda, F., Scatena, F.N. and Bruijnzeel, L.A. (2006). Characteristics of Fog and Fogwater Fluxes in a Puerto Rican Elfin Cloud Forest. *Agric. For. Meteorol.* 139: 288–306.

Fitzgerald, E., Ault, A.P., Zauscher, M., Mayol-Bracero, O.L. and Prather, K.A. (2015). Comparison of the Mixing State of Long-range Transported Asian and African Mineral Dust. *Atmos. Environ.* 115: 19–25.

García-Martinó, A.R., Warner, G.S., Scatena, F.N. and Civco, D.L. (1996). Rainfall, Runoff, and Elevation Relationships in the Luquillo Mountains of Puerto Rico. *Carib. J. Sci.* 32: 413–424.

Gioda, A., Mayol-Bracero, O.L., Morales-García, F., Reyes-Rodríguez, G.J., Santos-Figueroa, G. and Collett, Jr., J. (2008). Water-soluble Organic and Nitrogen Levels in Cloud and Rainwater in a Background Marine Environment under Influence of Different Air Masses. *J. Atmos. Chem.* 61: 85–99.

Gioda, A., Mayol-Bracero, O.L., Morales-García, F., Collett, J., Decesari, S., Emblico, L., Facchini, M.C., Morales-De Jesús, R.J., Mertes, S., Borrmann, S., Walter, S. and Schneider, J. (2009). Chemical Composition of Cloud Water in the Puerto Rican Tropical Trade Wind Cumuli. *Water Air Soil Pollut.* 200: 3–14.

Gioda, A., Reyes-Rodríguez, G.J., Santos-Figueroa, G., Collet Jr., J.L., Decesari, S., da Conceição, M., Ramos, K.V., Bezerra-Netto, H.J., de Aquino-Neto, F.R. and Mayol-Bracero, O.L. (2011). Speciation of Water-soluble Inorganic, Organic, and Total Nitrogen in a Background Environment: Cloud Water, Rainwater, and Aerosol Particles. *J. Geophys. Res.* 116: D05203, doi: 10.1029/2010JD015010.

Gioda, A., Mayol-Bracero, O.L., Scatena, F.N., Weathers, K.C., Mateus, V.L. and McDowell, W.H. (2013). Chemical Constituents in Clouds and Rainwater in the Puerto Rican Rainforest: Potential Sources and Seasonal Drivers. *Atmos. Environ.* 68: 208–220.

Haywood, J.M., Pelon, J., Formenti, P., Bharmal, N. Brooks, M., Capes, G., Chazette, P., Chou, C., Christopher, S., Coe, H., Cuesta, J., Derimian, Y., Desboeusfs, K., Greed, G., Harrison, M., Heese, B., Highwood, E.J., Johnson, B., Mallet, M., Marticorena, B., Marsham, J., Milton, S., Myhre, G., Osborne, S.R., Parker, J.D., Rajot, J.L., Schulz, M., Slingo, A., Tanre, D. and Tulet, P. (2008). Overview of the Dust and Biomass-burning Experiment and African Monsoon Multidisciplinary Analysis Special Observing Period-0. *J. Geophys. Res.* 113: D00C17, doi: 10.1029/2008JD010077.

Jones, P.D. and Moberg, A. (2003). Hemispheric and Large-scale Surface Air Temperature Variations: An Extensive Revision and an Update to 2001. *J. Clim.* 16: 206–223.

Keene, W.C., Pszenny, A.A.P., Galloway, J.N. and Hawley, M.E. (1986). Sea-salt Corrections and Interpretation of Constituent Ratios in Marine Precipitation. *J. Geophys. Res.* 91: 6647–6658.

Loope, L.L. and Giambelluca, T.W. (1998). Vulnerability of Island Tropical Montane Cloud Forests to Climate Change, with Special Reference to East Maui, Hawaii. *Clim. Change* 39: 503–517.

Lugo, A.E. and Scatena, F.N. (1992). Epiphytes and Climate Change Research: A Proposal. *Selbyana* 13: 123–130.

Manahan, S.E. (2000). *Environmental Chemistry 7th Ed.*, Lewis Publishers, Boca Raton, Florida, pp. 70–75.

Maring, H., Savoie, D.L., Izaguirre, M.A. and Custals, L. (2003). Mineral Dust Aerosol Size Distribution Change during Atmospheric Transport. *J. Geophys. Res.* 108: 8592, doi: 10.1029/2002JD002536.

Martens, C.S. and Harriss, R.C. (1973). Chemistry of Aerosols, Cloud Droplets, and Rain in the Puerto Rican Marine Atmosphere. *J. Geophys. Res.* 78: 949–957.

Olander, L.P., Scatena, F.N. and Silver, W.L. (1998). Global Climatic Change, Hurricanes, and a Tropical Forest. *Clim. Change* 22: 175–190.

Peden, M.E. (1983). *Sampling, Analytical, and Quality Assurance Protocols for the National Atmospheric Deposition Program*, Sampling and Analysis of Rain, ASTM STP 823, S.A. Campbell, Ed., pp. 72–83.

Pounds, J.A., Michael, P., Fogden, L. and Campbell, J.H. (1999). Biological Response to Climate Change on a Tropical Mountain. *Nature* 398: 611–615.

Possanzini, M., Buttini, P. and Dipalo, V. (1988). Characterization of a Rural Area in Terms of Dry and Wet Deposition. *Sci. Total Environ.* 74: 111–120.

Prospero, J.M. (1999). Long-range Transport of Mineral Dust in the Global Atmosphere: Impact of African Dust on the Environment of the Southeastern United States. *Proc. Natl. Acad. Sci. U.S.A.* 96: 3396–3403.

Prospero, J.M. and Lamb, P.J. (2003). African Droughts and Dust Transport to the Caribbean: Climate Change Implications. *Science* 302: 1024–1027.

Prospero, J.M. and Mayol-Bracero, O.L. (2013). Understanding the Transport and Impact of African Dust on the Caribbean Basin. *Bull. Am. Meteorol. Soc.* 94: 1329–1337.

Reyes-Rodríguez, G.J., Gioda, A., Mayol-Bracero, O.L. and Collett, Jr., J. (2009). Organic Carbon, Total Nitrogen, and Water-soluble Ions in Clouds from a Tropical Montane Cloud Forest in Puerto Rico. *Atmos. Environ.* 43: 4171–4177.

Rosenfeld, D., Rudich, Y. and Lahav, R. (2001). Desert Dust Suppressing Precipitation: A Possible Desertification Feedback Loop. *Proc. Natl. Acad. Sci. U.S.A.* 98: 5975–5980.

Scatena, F.N. (1995). Relative Scales of Time and Effectiveness of Watershed Processes in a Tropical Montane Rainforest of Puerto Rico. *Am. Geophys. Union Geophys. Monogr.* 89: 103–111.

Spiegel, J.K., Buchmann, N., Mayol-Bracero, O.L., Cuadra-Rodríguez, L.A., Valle-Díaz, C.J., Prather, K.A., Mertes, S. and Eugster, W. (2014). Do Cloud Properties in a Puerto Rican Tropical Montane Cloud Forest Depend on Occurrence of Long-range Transported African Dust? *Pure Appl. Geophys.* 171: 2443–2459

Stadtmüller, T. and Agudelo, N. (1990). Amount and Variability of Cloud Moisture Input in a Tropical Cloud Forest. *IAHS Publ.* 193: 25–32.

Still, C., Foster, P.N. and Schneider, S.H. (1999). Simulating the Effects of Climate Change on Tropical Montane Cloud Forests. *Nature* 398: 608–610.

Straub, D.J., Lee, T. and Collett Jr., J.L. (2007). Chemical Composition of Marine Stratocumulus Clouds over the Eastern Pacific Ocean. *J. Geophys. Res.* 112: doi: D04307, 10.1029/2006JD007439.

Sullivan, R.C., Moore, M.J.K., Petters, M.D., Kreidenweis, S.M., Roberts, G.C. and Prather, K.A. (2009). Effect of Chemical Mixing State on the Hygroscopicity and Cloud Nucleation Properties of Calcium Mineral Dust Particles. *Atmos. Chem. Phys.* 9: 3303–3316.

Sun, M., Wang, Y., Wang, T., Fan, S., Wang, W., Li, P., Guo, J. and Li, Y. (2010). Cloud and the Corresponding Precipitation Chemistry in South China: Water-soluble Components and Pollution Transport. *J. Geophys. Res.* 115: D22303, doi: 10.1029/2010JD014315.

Taylor, S.R. (1964). Abundance of Chemical Elements in the Continental Crust: A New Table. *Geochim. Cosmochim. Acta* 28: 1273–1285.

Tuncer, B., Bayer, B., Yesilyurt, C. and Tuncel, G. (2001). Ionic Composition of Precipitation at the Central Anatolia, Turkey. *Atmos. Environ.* 35: 5989–6002.

Usher, C.R., Michel, A.E. and Grassian, V.H. (2003). Reactions on Mineral Dust. *Chem. Rev.* 103: 4883–4839.

Weathers, K.C., Likens, G.H., Bormann, F.B., Bicknell, S.H., Bormann, B.T., Daube, B.C., Eaton, J.S., Galloway, J.N., Keene, W.C., Kimball, K.D., McDowell, W.H., Siccama, T.G., Smiley, D. and Tarrant, R.A. (1988). Cloud Chemistry from Ten Sites in North America. *Atmos. Environ.* 22: 1018–1026.

Weaver, P.L. (1972). Cloud Moisture Interception in the Luquillo Mountains of Puerto Rico. *Carib. J. Sci.* 12: 129–144.

Weaver, P.L. (1990). Succession in the Elfin Woodland of the Luquillo Mountains of Puerto Rico. *Biotropica* 22: 83–89.

Wilson, T.R.S. (1975). *Salinity and the Major Elements of Seawater, in Chemical Oceanography*, 2nd Edition, Riley, J.P. and Skirrow, G. (Eds.), vol. 1, 2nd ed., Academic, Orlando, Fla, pp. 365–413.

Yu, J.Z., Huang, X.F., Xu, J. and Hu, M. (2004). When Aerosol Sulfate Goes Up, So Does Oxalate: Implication for the Formation Mechanisms of Oxalate. *Environ. Sci. Technol.* 39: 128–133.

Received for review, June 1, 2015
Revised, September 18, 2015
Accepted, December 9, 2015